Chapter 1. Global agroclimatic patterns

Chapter 1 describes the CropWatch agroclimatic indicators for rainfall (RAIN, figure 1.1), temperature (TEMP, figure 1.2), and radiation (RADPAR, figure 1.3), along with the agronomic indicator for potential biomass (BIOMSS, figure 1.4) for sixty-five global Monitoring and Reporting Units (MRU). Rainfall, temperature, and radiation indicators are compared to their average value for the same period over the last thirteen years (called the "average"), while BIOMSS is compared to the indicator's average of the recent five years. Indicator values for all MRUs are included in Annex A, table A.1. For more information about the MRUs and indicators, please see Annex C and online CropWatch resources at ww.cropwatch.com.cn.

1.1 Overview

Over the current reporting period—October 1 2014 to January 31 2015, global agroclimatic patterns are characterized by a significant deficit of sunshine in the northern hemisphere and India, along with an occurrence of coherent rainfall patterns in several regions.

The northern hemisphere sunshine deficit consisted of a more than 3% drop below average for radiation in most areas above 20 degrees northern latitude and in India; only an area from the Ukraine to the Ural mountains (MRU-58) and the Lower Yangtze (MRU-37) were excepted, with both areas showing normal conditions. With the exception of the Brazilian Nordeste (MRU-22) and the Gulf of Guinea region (MRU-03), radiation was higher than expected in equatorial regions and southern Africa, including all of Southeast Asia and southern Africa.

The largest radiation deficits occurred in the Ural to Altai mountains (MRU-62, -10%) and—among the major crop producing areas—in non-Mediterranean Western Europe (MRU-60, -8%) andCorn Belt (MRU-13, -6%). The highest positive departures for radiation are those of Equatorial central Africa (MRU-01) and Central-eastern Brazil (MRU-23), both showing 7% above average sunshine.

The typical rainfall patterns include deficits on the eastern margin of Asia and Oceania, Africa, and South America. In Asia and Oceania, rainfall extremes occurred in southern Japan and Korea (MRU-46,-33%), Hainan (MRU-33, -55%), Taiwan (MRU-42, -84%), and New Zealand (MRU-56, -69%), but also affected other Chinese regions (Lower Yangtze MRU-37, -28%) and maritime Southeast Asia (MRU-49, -5%). In Africa, the effect is most marked in the Horn of Africa (MRU-04,-23%) and southwest Madagascar (MRU-06,-31%), but less so in the east African highlands (MRU-02, -8%) and southern Africa (MRU-09, -5%). Finally, in South America, the Nordeste (MRU-22, -27%) and the extreme south (MRUs 27 and 28) stand out with values between -28% and -60%. In contrast, the Pampas MRU (MRU-26), a major agricultural area, benefited from above-average rainfall (+26%).

Finally, favorable conditions for rainfall existed in a large area in Asia stretching from Huanghuaihai (MRU-34, +44%) and Southwest China (MRU-41, +81%) across much of central Asia to the Ural to Altai mountains (MRU-62, +52%), showing large rainfall departures of above 50%, including the record for the current reporting period: +413% in southern Mongolia (MRU-47).

1.2 Rainfall

Over the monitoring period, almost all summer crops were harvested, and winter crops were planted in the northern hemisphere. In the southern hemisphere, the harvest season is either nearing completion or already finished. Rainfall showed a large variation across regions (figure 1.1).

Overall, the southern hemisphere suffered insufficient rainfall, including the Western Cape (MRU-10, -60%), southwest Madagascar (MRU-06, -31%), Horn of Africa (MRU-04,-23%), Nordeste (MRU-22, -27%),

Amazon (MRU-24, -19%), central-eastern Brazil (MRU-23, -17%), New Zealand (MRU-56, -69%), and northern Australia (MRU-53, -13%). Fortunately, the rainfall amounts in the main production zones in the southern hemisphere were close to normal or above average, including in the Pampas (MRU-26, +30%), Queensland to Victoria (MRU-54, +6%), and the Gulf of Guinea (MRU-03, +5%). Most other regions had close to average rainfall, such as North African-Mediterranean (MRU-07, -5%).

The variation of rainfall in the northern hemisphere is complicated. In North America, except for the West Coast (MRU-16, -18%), abundant or average rainfall occurred in the Corn Belt (MRU-13, +4%), British Columbia to Colorado (MRU-11, +44%), northern Great Plains (MRU-12, +54%), and the area extending from the Cotton Belt to Mexican Noreste (MRU-14, +17%). In China, although rainfall in the Lower Yangtze (MRU-37) was 28% below average, abundant rainfall fell over Huanghuaihai (MRU-34, +44%), the Loess region (MRU-36, +34%), Northeast China (MRU-38, +28%), and Southern China (MRU-40, +20%). Insufficient rainfall was recorded in the MRUs of East Asia (MRU-43, -25%) and southern Japan and Korea (MRU-C46, -33%).

In the main rice production zones, rainfall was close to average in Southeast Asia and South Asia, including mainland Southeast Asia (MRU-50, +0%), southern Himalayas (MRU-44, +9%), southern Asia (MRU-45, +6%), Punjab to Gujarat (MRU-48, -9%), and maritime Southeast Asia (MRU-49, -5%).

Rainfall was normal in Western Europe (MRU-60, +4%) and the Ukraine to Ural mountains (MRU-58, -6%), but insufficient rainfall fell over Mediterranean Europe and Turkey (MRU-59, -18%). In central Asia, abundant rainfall fell over the Ural to Altai mountains area (MRU-62, +51%).

Figure 1.1. Global map of rainfall anomaly (as indicated by the RAIN indicator) by MRU, departure from 13YA, October 2014-January 2015 (percentage)

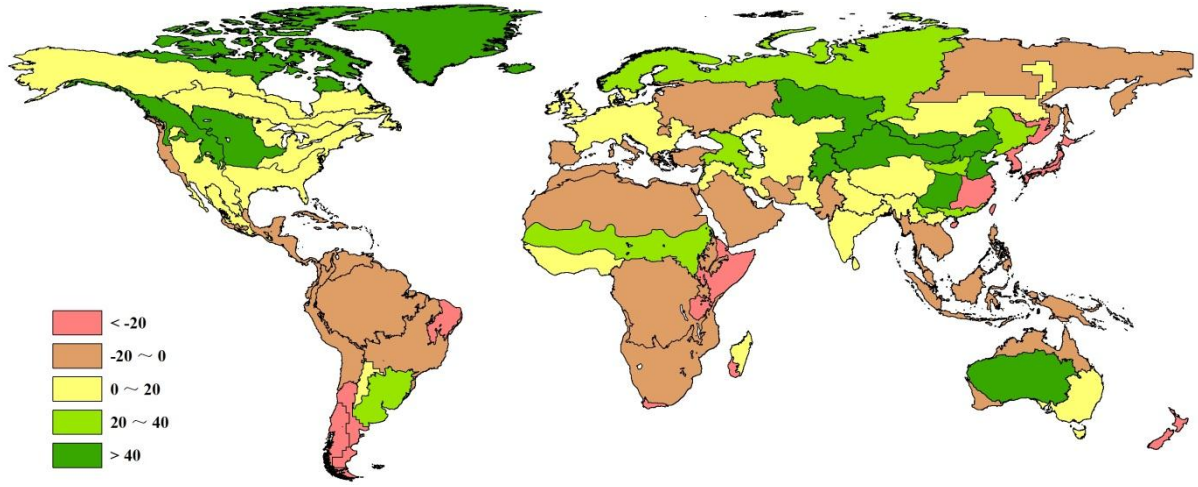

Note: Data for October 2014-January 2015, compared with the thirteen-year average (13YA) for the same period 2001-2013.

1.3 Temperature

Over the reporting period, most parts of the world experienced average temperature (TEMP) conditions compared to average (figure 1.2). In North America, temperature was above average in the west and below average in the east. The greatest positive temperature departures are found on the West Coast (MRU-16, +2.2°C) and in an area from British Columbia to Colorado (MRU-11, +1.7°C). In the non-agricultural sub-boreal America (MRU-15, -0.8°C) average temperature was -7.9°C, while precipitation was abundant (RAIN, +9%). In South America and Africa, most MRUs were warmer than usual, with the exception of western Patagonia (MRU-27, -0.4°C). In Oceania, below average temperatures were found in the Australian desert (MRU-63, -0.7) and Queensland to Victoria (MRU-54, -0.5°C).

Among the areas that were warmer than average, many are found in Eurasia, with the largest positive departure in non-Mediterranean Western Europe (MRU-60, +2.1°C). In Ukraine to Ural Mountains (MRU-58, -0.3°C) and Ural to Altai mountains (MRU-62, -0.5), the temperature was below the average and lower than 0°C.

Figure 1.2. Global map of air temperature anomaly (as indicated by the TEMP indicator) by MRU, departure from 13YA, October 2014-January 2015 (degrees Celsius)

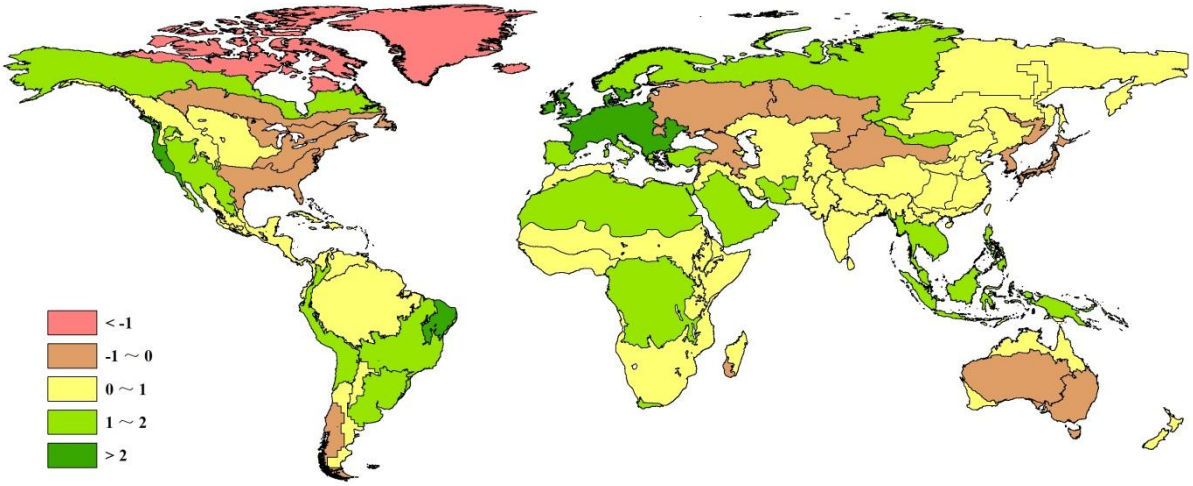

Note: Data for October 2014-January 2015, compared with the thirteen-year average (13YA) for the same period 2001-2013.

1.4 Photosynthetically active radiation

The observed photosynthetically active radiation assessed by the RADPAR CropWatch agroclimatic indicator was mostly consistent with rainfall and temperature mentioned above (see figure 1.3). Compared to average, most MRUs in the northern hemisphere showed below average values, while in the southern hemisphere most were above average. The highest increases compared to average (+7%) occurred in both equatorial central Africa (MRU-01) and central eastern Brazil (MRU-23). The Amazon region also experienced above average PAR (+5%). Record low radiation departures were concentrated in the North American continent and mainland Europe, including (i) Corn Belt (MRU-13, -6%), sub-boreal America (MRU-15, -6%), and boreal America (MRU-61, -5%); (ii) Western Europe (MRU-60, -8%) and Ural to Altai mountains (MRU-62, -10%); and (iii) boreal Eurasia (MRU-57) where the absolute highest PAR departure from the recent reference period occurred (-14%). While the mentioned northernmost areas do not play a significant role in agricultural production, their PAR values underscore the spatial coherence of PAR variations.

Most regions of China show a decrease in radiation. The major winter wheat production area in Huanghuaihai (MRU-34, -3%) and the Loess region (MRU-36, -4%) show a significant decrease in RADPAR, which may have negative effects on the growth of winter wheat. The largest negative departure in China was recorded in Gansu-Xinjiang (MRU-32, -5%), which resulted from abundant rainfall in this region.

Figure 1.3. Global map of PAR anomaly (as indicated by the RADPAR indicator) by MRU, departure from 13YA, October 2014-January 2015 (percentage)

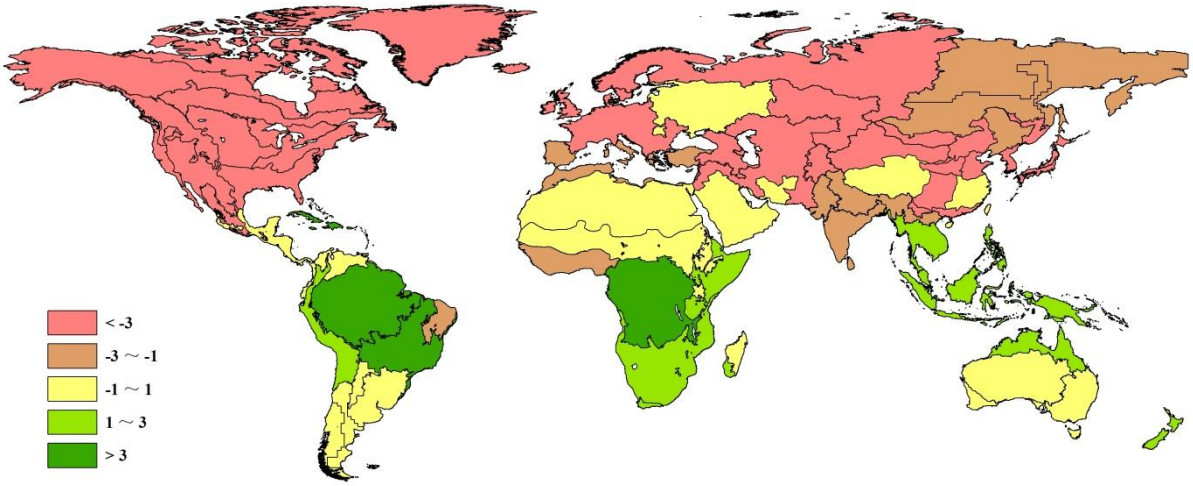

Note: Data for October 2014-January 2015, compared with the thirteen-year average (13YA) for the same period 2001-2013.

1.5 Biomass

BIOMSS is a synthetic agro-climatic indicator that takes into account rainfall and temperature to estimate the potential biomass accumulation. Recent departures from average for the 65 global MRUs are shown in figure 1.4.

Figure 1.4. Global map of biomass accumulation (BIOMSS) by MRU, departure from 5YA, October 2014-January 2015 (percentage)

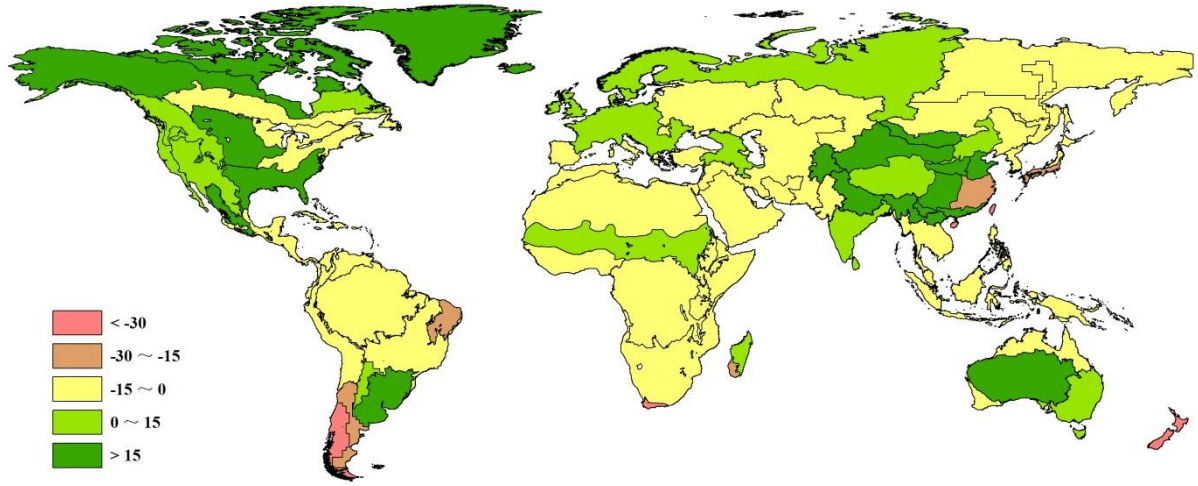

Note: Data for October 2014-January 2015, compared with the five-year average (5YA) for the same period 2009-2013.

Overall, 27 MRUs display a potential biomass accumulation during the October 2014 to January 2015 monitoring period that is higher than in other areas for the same period, usually due to high temperatures and abundant precipitation. The greatest positive biomass accumulation departures are found in the Australian desert (MRU-63, +23%), boreal America (MRU-61, +24%), southern Himalayas (MRU-44, +26%), northern Great Plains (MRU-12, +37%), Gansu-Xinjiang (MRU-32, +42%), Southwest China (MRU-41, +59%), southern Mongolia (MRU-47, +167%), and sub-arctic America (C65, +226%). At the scale of the MRUs, large negative BIOMSS departures occur in the Nordeste (MRU-22, -23%), lower Yangtze (MRU-37, -24%), southwest Madagascar (MRU-6, -29%), western Patagonia (MRU-27,-47%), Hainan (MRU-33,-51%), Western Cape (MRU-10,-52%), New Zealand (MRU-56,-57%), and Taiwan (MRU-42,-77).